

Determination of time-lapse perturbations directly from differenced seismic reflection data

Kris Innanen and Mostafa Naghizadeh

ABSTRACT

Scattering theory is a natural framework within which to directly pose the time-lapse seismic inverse problem. Within that theory, if time-lapse difference data are identified with the scattered field, the perturbation becomes a direct measure of the time-lapse acoustic/elastic property and structural changes within the Earth volume of interest. A wave-theoretic relationship of this kind, free of nonphysical artifacts, is not easy to deduce otherwise: think of propagating a 2-way wave through a difference model with a single mobile interface, and the spurious multiples that would be created between the interface and *itself at a later time*. The main complication in the scattering description lies in the heterogeneity of the reference medium, which generates roughly as many reflections as the perturbed medium. Since most existing inverse scattering imaging/inversion methods assume a smooth, non-reflecting reference, the problem would appear to require a complete reformulation. Doing this provides us with both inversion methods of increased accuracy, and an explanation of why inconsistently posed methods do better than one might imagine they should. The complicating influence of the heterogeneous reference medium is suggestive that inversion be considered within certain special cases: multidimensional structural inversion within the linearized regime only, and linear or nonlinear inversion when analyzing a single isolated primary event to determine mechanical property variations within a known, fixed target.

INTRODUCTION

The objectives of this paper are to (1) identify and examine some basic mathematical and geophysical issues arising in the time-lapse seismic inverse problem when it is described using scattering or perturbation theory, and (2) use the same framework to form direct inverse procedures applicable to several special but important cases of time-lapse imaging and inversion.

A *standard* (hereafter taken to mean *non time-lapse*) seismic reflection survey involves data measured along a time dimension and several space dimensions. A time-lapse, or 4D, survey (e.g., Greaves and Fulp, 1987; Lumley, 2001; Arts et al., 2004) introduces a second, “calendar” time dimension along which the standard seismic survey is repeated, such that the evolution of a given volume of Earth may be characterized over monthly, yearly, or even decade-length time scales. There are at least two seismic experiments involved in a time-lapse survey: the baseline survey, followed by one or more monitoring surveys. The “difference data” are the data formed by subtracting the baseline survey data from the monitoring survey data, and the “difference model” is the spatial distribution of Earth mechanical/impedance property differences that have accrued from the time of the baseline survey to the time of the monitoring survey. In that interval, several important geological/geophysical changes may have occurred: a target of interest may have undergone significant fluid content or pressure alteration, while remaining fixed spatially, e.g.,

under caprock; or, a target's boundaries may have migrated, if it is a fluid or gas plume; or, indeed, both the location and mechanical property contrasts of a boundary may have undergone significant change.

The difference data are sensitive to the difference model; this may be exploited to aid in monitoring of reservoir evolution. For instance, AVO/AVA inversion, a well-known framework for seismic parameter estimation, has been specifically tailored to the time-lapse problem by Landro (2001), who derived linearized expressions for the difference reflection coefficient of an interface between the monitoring and baseline surveys, and used them to discriminate between target pressure and fluid changes.

Scattering theory as applied to seismic reflection data (Weglein et al., 2003), and perturbation theory in general, would appear to have significant potential as a framework upon which to derive time-lapse inverse procedures. The potential has remained thus far almost, but not quite, completely unrealized. The essential idea, as advocated by Zhang (2006), is to identify the reference medium with the reservoir at the time of the baseline survey, and the perturbed medium with the reservoir at the time of the monitoring survey. With this basic identification in place, several possible routes are available, including that of directly applying, or “porting”, an existing inverse scattering algorithm, derived with non time-lapse assumptions, straight onto time-lapse difference data. This approach was taken by the originating researchers (Zhang, 2006).

The above identification does, however, introduce enough new issues to invite a complete reformulation of the problem, which is the approach we take in this paper. Let us begin, though, by confronting a compelling reason *not* to do so, which is that it is a highly complicated enterprise, as a consequence of the baseline survey/reference medium connection. Unlike in standard inverse scattering theories, in which we are free to choose the properties of the reference medium to suit our needs, in a time-lapse setting the reference medium (i.e., the Earth volume at the time of the baseline survey) is a fixed thing, and is in general no less complex than the perturbed medium. In a scattering description, we are assumed to have precise knowledge of the wave field everywhere in the reference medium, and a requirement for that level of detailed baseline information could present difficulties.

A further issue, also closely related to the complexity of the reference medium, raises concerns about applying a ported inverse scattering method, in particular for imaging structural changes. A comparison of the assumptions of existing inverse scattering imaging/inversion methods with the nature of time-lapse data reveals rather dramatic inconsistencies. Inverse scattering algorithms involve very simple reference media, which, though they may be spatially heterogeneous, never diffract or reflect wave energy. Yet a reservoir at the time of a baseline survey certainly does, in fact the reflections in the baseline survey data set form roughly half of the events in the difference data, and these events are just as important as those of the monitoring survey. A key assumption within all mature inverse scattering seismic imaging and inversion algorithms, then, expressly rejects data of the kind time-lapse surveys produce. Existing imaging/inversion algorithms should surely not, therefore, be expected to easily port to time-lapse applications.

Against these concerns, however, we may set some published reports, and simple ini-

tial numerical experiments. Interestingly, the presumption that existing methods will not port does not seem to be borne out in practice. First, in the case of the recovery of time-lapse contrast differences, the aforementioned study (Zhang, 2006), which involved a direct nonlinear inversion algorithm that was derived under standard scattering assumptions, was reported as generating clear added value. Secondly, and quite strikingly, the apparent problem of reflections coming from a reference medium that is assumed to be smooth *simply does not appear*, when the idea is put to a linear test. Consider the simple example illustrated in Figure 1. A time-lapse experiment is devised in which we monitor the progression of a single subsurface interface as it migrates upward (left column, top panel then middle panel). The two seismic surveys (baseline and monitoring) consist of one spike wave at normal incidence on the interface at each of the two times, hence the reflection data consist of a single reflected primary during the baseline survey (middle column, top panel) and a similar primary at a slightly earlier time during the monitoring survey (centre panel). Each of these two data sets can individually be treated with a simple, linearized inverse scattering algorithm to recover the approximate character of the interface at each time. This is carried out in the right column, top panel followed by the middle panel of the same column. If a homogeneous reference medium is chosen, the recovery takes the form of “trace-integration” (Bleistein et al., 2000; Weglein et al., 2003), wherein the interface profile is seen to be proportional to the anti-derivative of the primary data. In this example, a linear scattering treatment of the time-lapse problem would have us take the difference of the two survey data-sets (middle column, bottom panel), identify the result as the scattered field, and invert this for the difference model. And indeed, doing so (i.e., again applying a simple homogeneous reference medium trace integration procedure, derived through non time-lapse assumptions) reconstructs very faithfully the “bump” representing the change in the interface location (bottom right panel). This suggests we may have been premature in worrying about the use of standard inverse scattering methods for the time-lapse problem.

But, we have not reconciled this positive result with our previous concerns, which still stand. The bump we have constructed requires both events in the difference data, one to “turn on” the bump as the trace is integrated from left to right, and the other to turn it back off. The latter event comes from the reflector in the reference medium. But the method we used assumed a homogeneous reference medium, which gives rise to no reflections. How could we be getting the right answer, if half of the data do not exist from the point of view of the inverse theory? We are left with the unnerving sense that although ported inverse scattering methods can generate useful estimation and inversion methods, the theory with which those methods are derived sheds no light on why they work.

We surmise, and choose as a starting point for the current research, that there likely exist certain special cases of seismic time-lapse monitoring, meaning particular subtypes of the seismic inverse problem (e.g., AVO inversion of a single interface), or certain regimes of small perturbation, in which (1) consistently posed time-lapse scattering theory might lead to practical and robust monitoring algorithms, and (2) inconsistently posed time-lapse scattering theory (i.e., based on standard scattering assumptions) might form approximate, and still practically useful, algorithms. And we set as our objectives not only the task of deriving and examining some of these algorithms, but additionally explaining how (2) could be, in light of the apparent contradiction above.

A key set of issues that we will *not* specifically address in this paper concerns the pre-processing that is commonly necessary to generate a meaningful comparison between baseline and monitoring surveys. This is particularly important when data sets of significantly different “vintage” are considered (Stucci et al., 2005). Pre-processing often includes re-datuming (Winthaege et al., 2004) or image registration (Fomel and Jin, 2009), wherein source/receiver locations and image features are aligned prior to interpretation, and also an attempt is made to distinguish between actual Earth volume changes from changes in, e.g., acquisition from survey to survey. Towards coping with the latter issue, Berkhout and Verschuur (2007) have posed the time-lapse problem in terms of a feedback filter model, showing that time-lapse acquisition differences and target/overburden differences may be distinguished therein. In this paper we will consider an idealized time-lapse experiment, wherein data are perfectly comparable from the baseline to the monitoring surveys, and we will only consider questions that remain nevertheless. However, as we describe in a companion paper (Naghizadeh and Innanen, 2010), we are investigating an approach to some of these preprocessing issues that is fully integrated with the scattering description, through a least-squares scheme (implemented for non time-lapse seismic imaging by Kaplan et al., 2010b,a). Least-squares methods comprise a promising line of attack that has shown merit in time-lapse applications elsewhere, for instance in joint inversion of baseline and monitoring data sets (Ayeni and Biondi, 2010).

This paper is organized as follows. In section 2, which is the longest of the sections in this paper, we carry out an initial analysis of the time-lapse problem under highly specialized and simple conditions: a scalar (e.g., acoustic and constant density) baseline medium, consisting of a single interface, i.e., two homogeneous halfspaces separated by a boundary, and a perturbation in which that boundary is changed either in amplitude or position. Data, measured above the interface, are due to a normally incident spike wave. Within this simple framework, we consider two cases in turn; first, the case of an immobile interface whose amplitude changes over calendar time, and second, a fixed-amplitude boundary whose position migrates over calendar time. For each of these cases we formulate the associated scattering quantities and explicitly calculate the resulting scattering series terms for the fields. Analysis of these terms provides insight into (1) the forming of time-lapse inverse procedures in more complex, realistic problems involving multiple dimensions and variations in multiple parameters, and (2) the origin and resolution of the apparently contradictory thought experiments we have contrived so far. In section 3 we extend the ideas developed in the mobile interface analysis to formulate a linearized scheme for direct multi-dimensional imaging of time-lapse difference data, and in particular connect the discussion to our companion discussion (Naghizadeh and Innanen, 2010). In section 4 we extend the ideas developed in the amplitude varying interface component of the initial analysis, to formulate linear and nonlinear inverse procedures by which the difference reflection coefficient is inverted directly for time-lapse perturbations in multiple parameters.

INITIAL ANALYSIS: 1D SINGLE-PARAMETER ACOUSTIC MEDIA

All of the basic questions we have posed regarding a perturbative treatment of time-lapse seismic monitoring data may be satisfactorily answered through a study of a single-parameter acoustic medium, varying in depth only, and illuminated by a normally-incident plane source. These initial results will be built on in the later sections to derive practical

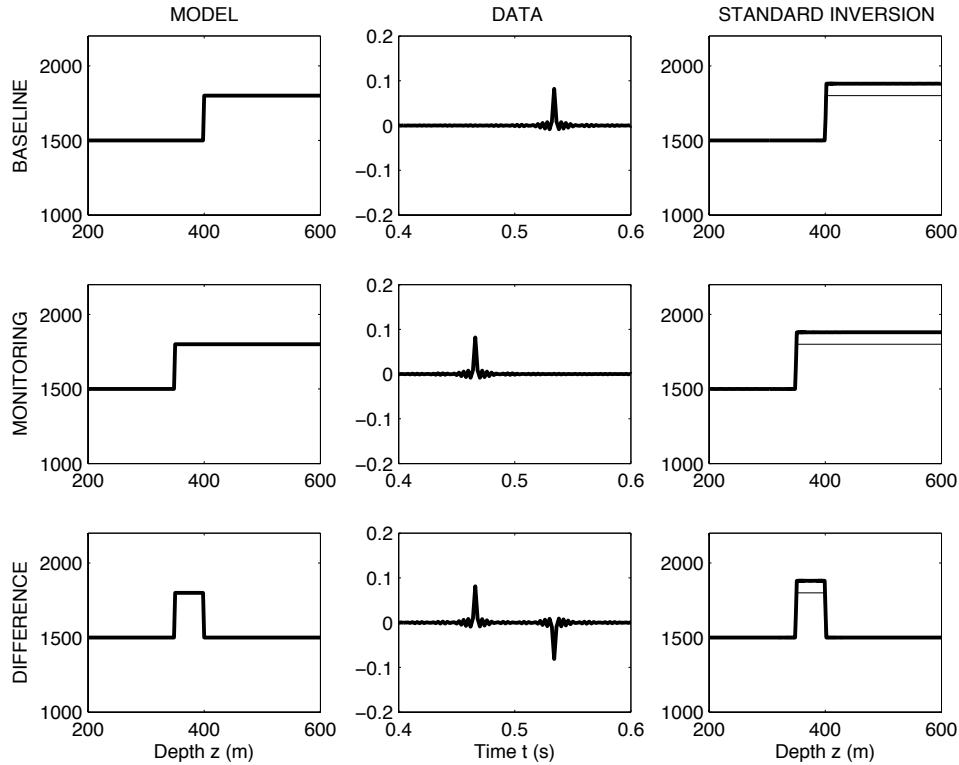


FIG. 1. Simple standard linearized inverse scattering algorithm applied to time-lapse data. Left column, top to bottom: baseline model, monitoring model, difference model. Middle column, top to bottom: baseline data, monitoring data, difference data. Right column: standard linearized inverse scattering applied to, top to bottom: baseline data, monitoring data, difference data. The *correctness* of the recovered difference model, in the bottom right panel, represents a pedagogical mystery: how can an algorithm unaware of the existence of the lower event use it to such good effect?

multidimensional and multi-parameter time-lapse inversion/monitoring algorithms.

Scattering from an amplitude-perturbed interface

In this first part of the initial analysis, we will treat the problem of a single interface in a constant density acoustic medium whose impedance varies from the time of the baseline survey to the time of the monitoring survey. The nonlinear relationship between the difference model and the difference data (in this case, the differenced impedance and the differenced reflection coefficient respectively) is developed, as is the linear approximation to the relationship. This analysis forms the basis for a time-lapse specific form of AVO/AVA inversion. Also, within the linear regime, we point out that an equivalence exists between this time-lapse problem and a notional non time-lapse scattering problem. This equivalence will later be extended and used to explain the apparent contradiction depicted in Figure 1.

Wave equations

We consider waves propagating in a reference medium composed of two scalar acoustic half-spaces separated by a single interface at depth z_1 (Figure 2, left panel). Anticipating a reflection-type wave experiment, we refer to the half-space above z_1 as the incidence

medium and below z_1 as the target medium. Overall waves propagate in this medium according to

$$\left[\frac{d^2}{dz^2} + \frac{\omega^2}{c_I^2(z)} \right] G(z, z_s, \omega) = \delta(z - z_s), \quad (1)$$

where

$$\frac{1}{c_I^2(z)} = \begin{cases} c_I^{-2}, & z > z_1 \\ c_0^{-2}, & z < z_1 \end{cases} \quad (2)$$

and c_0 and c_I are constants, with c_0 the incidence medium wavespeed and c_I the target wavespeed. We also consider waves that propagate in a second, perturbed, medium (Figure 2, right panel), with exactly the same structure but with the target medium altered from c_I to c_F , according to

$$\left[\frac{d^2}{dz^2} + \frac{\omega^2}{c_F^2(z)} \right] P(z, z_s, \omega) = \delta(z - z_s), \quad (3)$$

where

$$\frac{1}{c_F^2(z)} = \begin{cases} c_F^{-2}, & z > z_1 \\ c_0^{-2}, & z < z_1 \end{cases} . \quad (4)$$

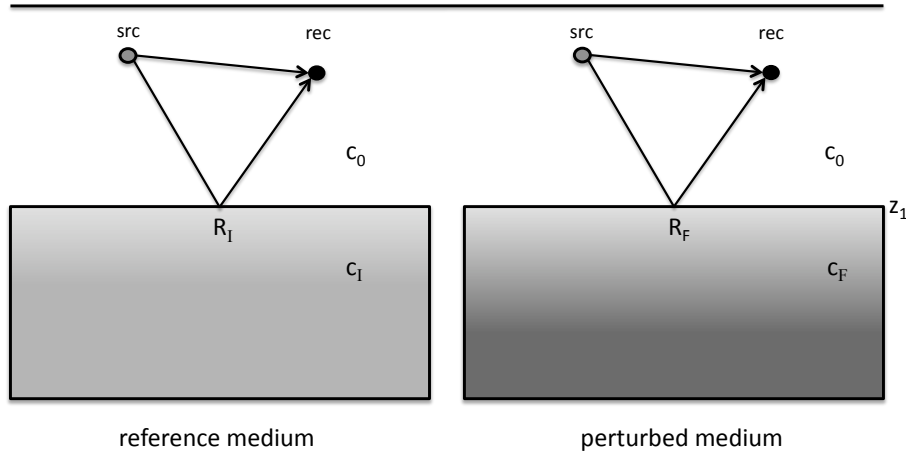


FIG. 2. Illustration of the reference and actual media in the problem of scattering from an amplitude-perturbed interface.

Green's functions

If the equations in the previous section are satisfied, propagation of the reference wave from z_s to z_g when both are within the incidence medium (i.e., $z_g, z_s < z_1$, as in Figure 3, left panel) takes the form:

$$G_{00}(z_g, z_s, \omega) = \frac{e^{ik_0|z_g - z_s|}}{i2k_0} + R_I \frac{e^{ik_0(z_1 - z_g)} e^{ik_0(z_1 - z_s)}}{i2k_0}, \quad (5)$$

where $k_0 = \omega/c_0$ and $R_I = (c_I - c_0)/(c_I + c_0)$. Propagation from z_s to z_g when both are within the reference target medium (i.e., $z_g, z_s > z_1$, as in Figure 3, right panel) takes the form:

$$G_{11}(z_g, z_s, \omega) = \frac{e^{ik_1|z_g-z_s|}}{i2k_1} - R_I \frac{e^{ik_1(z_g-z_1)}e^{ik_1(z_s-z_1)}}{i2k_1}, \quad (6)$$

where $k_1 = \omega/c_1$. Propagation from z_s to z_g , with z_s in the incidence medium and z_g in the reference target medium (i.e., $z_g > z_s$, as in Figure 3, middle panel) takes the form:

$$G_{01}(z_g, z_s, \omega) = T_D e^{ik_0(z_1-z_s)} \frac{e^{ik_1(z_g-z_1)}}{i2k_0}, \quad (7)$$

where $T_D = 2c_1/(c_0 + c_1)$ is the transmission coefficient downward across the z_1 boundary. Propagation from z_s to z_g with z_s in the reference target medium and z_g in the incidence medium (i.e., $z_g < z_s$, as in Figure 3, middle panel), takes the form:

$$G_{10}(z_g, z_s, \omega) = T_U e^{ik_1(z_s-z_1)} \frac{e^{ik_0(z_1-z_g)}}{i2k_1}, \quad (8)$$

where $T_U = 2c_0/(c_0 + c_1)$ is the transmission coefficient upward across the z_1 boundary.

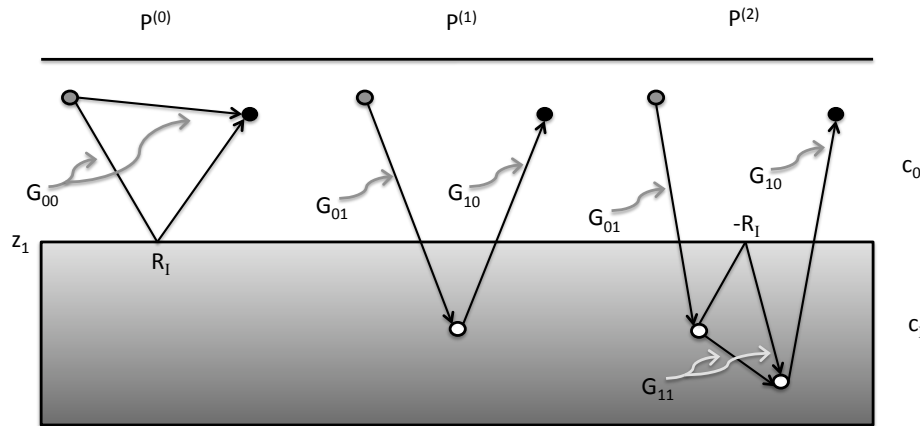


FIG. 3. Illustration of the action of the 1-interface Green's functions (equations 5–8) within the 0th, 1st and 2nd order terms of the time-lapse wave calculation.

Solutions

Finally, let us define a dimensionless perturbation

$$\begin{aligned} \alpha_{TL}(z) &= \begin{cases} 0, & z < z_1 \\ 1 - \frac{c_I^2}{c_F^2}, & z > z_1 \end{cases} \\ &= \alpha_{TL} H(z - z_1), \end{aligned} \quad (9)$$

where H is the Heaviside function and $\alpha_{TL} = 1 - c_I^2/c_F^2$ is a perturbation amplitude measuring the difference between the final and initial target medium properties c_I and c_F .

Taking the ω dependence as read, P in the reflection regime, i.e., $z_g, z_s < z_1$ is related to G and α_{TL} by a Born series constructed using the above framework:

$$P(z, z_s) = P^{(0)}(z, z_s) + P^{(1)}(z, z_s) + P^{(2)}(z, z_s) + \dots, \quad (10)$$

where, setting $z_g = z_s = 0$ for convenience, in the terminology of the Green's functions as we have defined them in equations (5)–(8),

$$P^{(0)} = G_{00}(0, 0), \quad (11)$$

$$P^{(1)} = \alpha_{TL} k_1^2 \int_{z_1}^{\infty} dz' G_{10}(0, z') G_{01}(z', 0), \quad (12)$$

$$P^{(2)} = \alpha_{TL}^2 k_1^4 \int_{z_1}^{\infty} dz' G_{10}(0, z') \int_{z_1}^{\infty} dz'' G_{11}(z', z'') G_{01}(z'', 0), \quad (13)$$

etc. Substituting the explicit forms for the Green's functions into these expressions and summing, we have

$$P = \left[1 + e^{i2k_0 z_1} \left(R_I + \frac{\alpha_{TL}}{4} T_D T_U + \frac{\alpha_{TL}^2}{16} T_D T_U (2 - R_I) + \dots \right) \right] \frac{1}{i2k_0}. \quad (14)$$

Consequently, the solution for what is typically referred to as the scattered field $P_S = P - G_0$, in the perturbed interface problem, has the form

$$P_S = \left(\frac{\alpha_{TL}}{4} + \frac{\alpha_{TL}^2}{16} (2 - R_I) + \frac{\alpha_{TL}^3}{64} (5 - 4R_I + R_I^2) + \dots \right) T_D T_U \frac{e^{i2k_0 z_1}}{i2k_0}. \quad (15)$$

All non-zero scattering contributions to P at second order and beyond have involved at least some propagation paths occurring entirely in the target medium, hence, through the Green's functions appropriate for those regions, the reference transmission coefficients T_U and T_D and a multiplicity of instances of the reference reflection coefficient R_I are incorporated in the solution.

Time-lapse interpretation

Let us suppose that the reference medium $c_I(z)$ corresponds to an Earth volume at the time of the baseline survey in a time-lapse experiment, and the medium $c_F(z)$ corresponds to the same volume at the time of a monitoring survey. This might represent a horizon that remains at the same location during the time-lapse interval but that undergoes a change in impedance properties, perhaps due to a change in fluid content. The quantity P_S in equation (15), restricted to a measurement surface above the Earth volume of interest, corresponds to the time-lapse difference data.

The phase of the field P_S in equation (15) is, as expected, that of a reflected wave propagating a distance $2z_1$. We interpret the amplitude terms as acting to correct the reference (baseline) reflection coefficient R_I to produce the actual (monitoring) reflection coefficient $R_F = (c_F - c_0)/(c_F + c_0)$:

$$R_F = R_I + \frac{\alpha_{TL}}{4} T_D T_U + \frac{\alpha_{TL}^2}{16} T_D T_U (2 - R_I) + \frac{\alpha_{TL}^3}{64} T_D T_U (5 - 4R_I + R_I^2) + \dots, \quad (16)$$

or, expressing the transmission coefficients in terms of the reflection coefficient, i.e., $T_D = 1 + R_I$ and $T_U = 1 - R_I$, we have

$$R_S \equiv R_F - R_I = \frac{1}{4}\alpha_{TL} [1 - R_I^2] + \frac{1}{8}\alpha_{TL}^2 \left[1 - \frac{1}{2}R_I - R_I^2 + \frac{1}{2}R_I^3 \right] + \frac{5}{64}\alpha_{TL}^3 \left[1 - \frac{4}{5}(R_I + R_I^2 - R_I^3) - \frac{1}{5}R_I^4 \right] + \dots \quad (17)$$

The difference R_S between the reflection coefficient associated with the final state, R_F , and the initial state R_I , is expressible as a series in powers of α_{TL} and R_I . We may truncate equation (17) to come to a range of approximations of $R_S = R_F - R_I$. The accuracy of a set of these is illustrated in Figure 4. It appears to become particularly good after third order, for the range of initial and final target wavespeeds considered. However, the top right panel of Figure 4 reveals that there are also regions of c_I and c_F in which the linearization of R_S provides a very reasonable approximation.

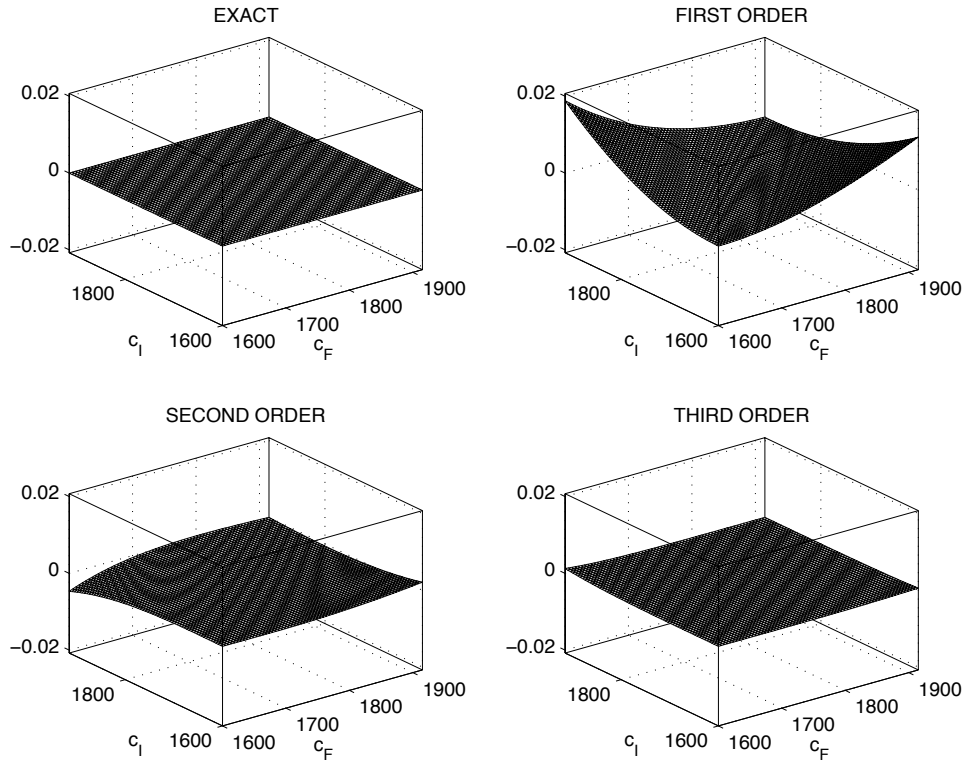


FIG. 4. Error plots for three approximations, first, second, and third order in α_{TL} , of equation (17). Each panel is calculated as the approximate R_S at a given order subtracted from the exact R_S for $c_0 = 1500$ m/s and a range of baseline/reference target P-wave velocities (c_I in m/s) and monitoring/perturbed target P-wave velocities (c_F in m/s). At first order regions of significant error are discernable, as are regions of relatively small c_I/c_F for which the approximation error is low. By third order in α_{TL} error is significantly reduced over the full range of c_I, c_F , plotted, but all three approximations are accurate within certain regimes of $c_I \approx c_F$.

Let us consider two special cases, first $R_I = 0$ and then $\alpha = 0$. If $R_I = 0$, the interface was not present during the baseline survey, when the Earth volume was in its initial state, and has appeared in the interim before the monitoring experiment. Then equation (17)

reduces to

$$R_S = R_F = \frac{1}{4}\alpha_{TL} + \frac{1}{8}\alpha_{TL}^2 + \frac{5}{64}\alpha_{TL}^3 + \dots, \quad (18)$$

where, since $c_I = c_0$ in this circumstance,

$$\alpha_{TL} = 1 - \frac{c_0^2}{c_F^2}. \quad (19)$$

This is the expected result, since the exact reflection coefficient at the final state is, in the same set of circumstances,

$$\begin{aligned} R_F &= \frac{c_F - c_0}{c_F + c_0} \\ &= \frac{1 - (1 - \alpha_{TL})^{1/2}}{1 + (1 - \alpha_{TL})^{1/2}} \\ &= \frac{1}{4}\alpha_{TL} + \frac{1}{8}\alpha_{TL}^2 + \frac{5}{64}\alpha_{TL}^3 + \dots \end{aligned} \quad (20)$$

More trivially if $\alpha_{TL} = 0$ it means the Earth volume is unchanged from initial to final state and $R_S = R_F - R_I$ is expected to be nil. This is the case, since all terms on the right hand side of equation (17) are at least first order in α .

Although R_I and α_{TL} are connected through their dependence on c_I , they are capable of varying independently, and they measure the “size” of different aspects of the time-lapse problem, respectively the size of the reference contrast and the size of the time-lapse contrast. Nevertheless if we are interested in the relative importance of terms in the series in equation (17), it makes sense to view them as combining to determine the order of a contribution to R_S . Let us re-define the order of a term in equation (17) as being the sum of the orders of α_{TL} and R_I , such that a term in $R_I^N \alpha_{TL}^M$ is order $N + M^*$. Doing so we see that R_S has a first order relationship with α_{TL} only, with R_I only appearing at second order and higher. That is, to first order

$$R_S \approx \frac{1}{4}\alpha_{TL}. \quad (21)$$

A comparison with the standard scattering problem.

Comparison of equations (20) and (21) reveals that to first order (in the combined α_{TL} , R_I sense), we have that $R_S = R_F$. This may be more instructively established by expanding R_S about the initial contrast causing R_I , for which we define $\alpha_S \equiv 1 - c_0^2/c_I^2$, in

*Note that in doing so we deviate from the ‘order’ implied by the superscripts in equation (10). In all formal scattering expressions in this paper, order refers to α_{TL} alone. Only in the “interpretive” sections do we make this re-assignment, at which point we will say so clearly.

addition to $\alpha_{TL} = 1 - c_I^2/c_F^2$:

$$\begin{aligned}
 R_S &= \frac{c_F/c_I - c_0/c_I}{c_F/c_I - c_0/c_I} - \left[\frac{1 - c_0^2/c_I^2}{1 + c_0^2/c_I^2} \right] \\
 &= \frac{(1 - \alpha_{TL})^{-1/2} - (1 - \alpha_S)^{1/2}}{(1 - \alpha_{TL})^{-1/2} + (1 - \alpha_S)^{1/2}} - \left[\frac{1 - (1 - \alpha_S)^{1/2}}{1 + (1 - \alpha_S)^{1/2}} \right] \\
 &\approx \left(\frac{1}{4}\alpha_S + \frac{1}{4}\alpha_{TL} \right) - \frac{1}{4}\alpha_S \\
 &= \frac{1}{4}\alpha_{TL},
 \end{aligned} \tag{22}$$

wherein the two terms have the same α_S dependence and opposite signs. We conclude that within this small R_I regime, the time-lapse scattering problem for a perturbed interface amplitude is equivalent to the scattering description of a standard problem involving a homogeneous reference medium c_0 and a contrast from c_0 to c_F . It follows that a standard *inverse* procedure, devised with this same homogeneous reference medium, will recover the correct time-lapse perturbation amplitude, again to first order.

Direct expansion of R_S .

The simplicity of the expression for the scattered field in equation (15) derives from the fact that the phase of the wave does not change from the time of the baseline survey to the time of the monitoring survey. The nonlinear scattering terms are, consequently, entirely concerned with the construction of the amplitude difference between R_I and R_F . Within this highly simplified environment, we may reproduce the same result with a certain kind of direct expansion of R_S . This will lead to considerable savings in effort in later sections when we consider multi-parameter problems of similar geometry.

The amplitude of the wave in equation (15) is R_S , where

$$\begin{aligned}
 R_S &= R_F - R_I \\
 &= \frac{c_F - c_0}{c_F + c_0} - R_I.
 \end{aligned} \tag{23}$$

Let us manipulate the first term on the right such that it may be expressed directly in terms of α_{TL} and α_S as defined previously:

$$\begin{aligned}
 R_F &= \frac{c_F/c_I - c_0/c_I}{c_F/c_I + c_0/c_I} \\
 &= \frac{(1 - \alpha_{TL})^{-1/2} - (1 - \alpha_S)^{1/2}}{(1 - \alpha_{TL})^{-1/2} + (1 - \alpha_S)^{1/2}},
 \end{aligned} \tag{24}$$

and expand in binomial series, obtaining

$$R_F = \frac{(1/2)\alpha_{TL} + (1/2)\alpha_S + (3/8)\alpha_{TL}^2 + (1/8)\alpha_S^2 + \dots}{2 + (1/2)\alpha_{TL} + (1/2)\alpha_S + (3/8)\alpha_{TL}^2 + (1/8)\alpha_S^2 + \dots}. \tag{25}$$

However, since R_I and α_S are related by

$$R_I = \frac{1 - c_0/c_1}{1 + c_0/c_1} = \frac{1}{4}a_S + \frac{1}{8}a_S^2 + \dots, \quad (26)$$

which can be inverted by forming the inverse series $\alpha_S = \alpha_{S_1} + \alpha_{S_2} + \dots$, in which α_{S_i} is i 'th order in R_I , substituting into equation (26), and equating like orders, we find we may express α_S directly in terms of R_I as

$$a_S = 4R_I - 8R_I^2 + \dots \quad (27)$$

Eliminating a_S in equation (25) in favour of R_I using equation (27), we have

$$\begin{aligned} R_F &= \frac{(1/4)\alpha_{TL} + (3/16)\alpha_{TL}^2 + R_I - R_I^2 + \dots}{1 + (1/4)\alpha_{TL} + (3/16)\alpha_{TL}^2 - R_I + R_I^2 + \dots} \\ &= R_I + \frac{1}{4}\alpha_{TL}(1 - R_I^2) + \frac{1}{8}\alpha_{TL}^2 \left(1 - \frac{1}{2}R_I - R_I^2\right) + \dots, \end{aligned} \quad (28)$$

which, when compared with equation (17), is seen to reproduce the terms generated by the full evaluation of the Born series integrals.

Inversion for an amplitude-perturbed interface.

In the general case R_I and α_{TL} are both non-negligible. With the full expression for R_S in hand, in equation (17), we may next consider the direct nonlinear time-lapse inverse problem. The set of procedures known collectively as the inverse scattering series (Weglein et al., 2003) has been cast to invert the information carried by a single reflection coefficient, both for acoustic/elastic problems (Zhang and Weglein, 2009a,b) and for an-acoustic/anelastic problems (Innanen, 2010). In the latter reference, following the approach discussed by (Innanen, 2008), the inversion was formulated beginning with the forward (Born) series construction of the reflection coefficient only. The two approaches lead to the same result, but the former is immediately applicable to the particular series in equation (17). Let us suppose that the contributions to R_S of terms of greater powers of α or R_I than $\alpha^2 R_I^2$ is negligible. That is,

$$R_S \approx \frac{1}{4}\alpha_{TL}(1 - R_I^2) + \frac{1}{8}\alpha_{TL}^2 \left(1 - \frac{1}{2}R_I - R_I^2\right). \quad (29)$$

We expand α_{TL} in series,

$$\alpha = \alpha_{TL_1} + \alpha_{TL_2} + \dots, \quad (30)$$

where α_{TL_i} as before is deemed to be the portion of α_{TL} that is i th order in R_S , and like orders are equated:

$$R_S = \frac{1}{4}\alpha_{TL_1}(1 - R_I^2) + \frac{1}{4}\alpha_{TL_2}(1 - R_I^2) + \frac{1}{8}\alpha_{TL_1}^2 \left(1 - \frac{1}{2}R_I - R_I^2\right) + \dots \quad (31)$$

$$R_S = \frac{1}{4}\alpha_{TL_1}(1 - R_I^2), \quad (32)$$

$$0 = \frac{1}{4}\alpha_{TL_2}(1 - R_I^2) + \frac{1}{8}\alpha_{TL_1}^2 \left(1 - \frac{1}{2}R_I - R_I^2\right). \quad (33)$$

Thereafter α_{TL_1} and α_{TL_2} are sequentially solved-for, and summed to form approximations of α_{TL} . To first order in R_S ,

$$\alpha_{TL} \approx \alpha_{TL_1} = 4R_S \left(\frac{1}{1 - R_I^2}\right), \quad (34)$$

and to second order

$$\alpha_{TL} \approx \alpha_{TL_1} + \alpha_{TL_2} = 4R_S \left(\frac{1}{1 - R_I^2}\right) - 8R_S^2 \left[\frac{1 - (1/2)R_I - R_I^2}{(1 - R_I^2)^3}\right]. \quad (35)$$

Standard inverse scattering methods applied to R_S lead instead to first and second order formulas:

$$\alpha_{TL} \approx 4R_S \quad (36)$$

$$\alpha_{TL} \approx 4R_S - 8R_S^2. \quad (37)$$

Equations (35) and (37) are equivalent if $R_I \approx 0$ as discussed in the previous section. Figures 5 and 6 illustrate the differences between inversion with the formulas in equations (34)–(37) for two values of the baseline target velocity: $c_I = 3950\text{m/s}$ and $c_I = 3150\text{m/s}$ respectively. In all cases, $c_0 = 1500\text{m/s}$, and we use the recovered α values to generate estimates of the monitoring target velocity c_F , plotted on the vertical axes against its exact counterpart on the horizontal axes. The bold solid lines are the results a perfect inversion would produce, i.e., a line with unit slope. The top rows represent linearized inversions (linear with respect to R_S): the results of equation (34), solid, and equation (36), dashed. The left panels plot a range of recovered c_F values that are low with respect to the current value of the baseline target velocity c_I , and the right panels plot relatively high c_F values. The bottom rows are a repeat of the exercise, but inverting with the nonlinear formulas in equation (35), solid, and in equation (37), dashed. In all cases for a large c_I such as this, the importance of posing the time-lapse problem consistently, as in equations (34)–(35), is clear, though the standard results are seen to be of very reasonable accuracy, even to the point (e.g., left column, Figure 5) where incorporating the nonlinear correction, and not the R_I terms, makes a consistent improvement to the inversion. Interestingly, in the top right panel of Figure 6, we notice that the standard inverse result is an improvement over the correctly-posed time-lapse result, although the consistently posed version of the problem recovers its place in top spot by the time the second order correction is included (bottom right panel of Figure 6).

Scattering from a depth-perturbed interface

In this second part of the initial analysis, we will treat the problem of a single interface in a constant density acoustic medium whose depth changes from the time of the baseline

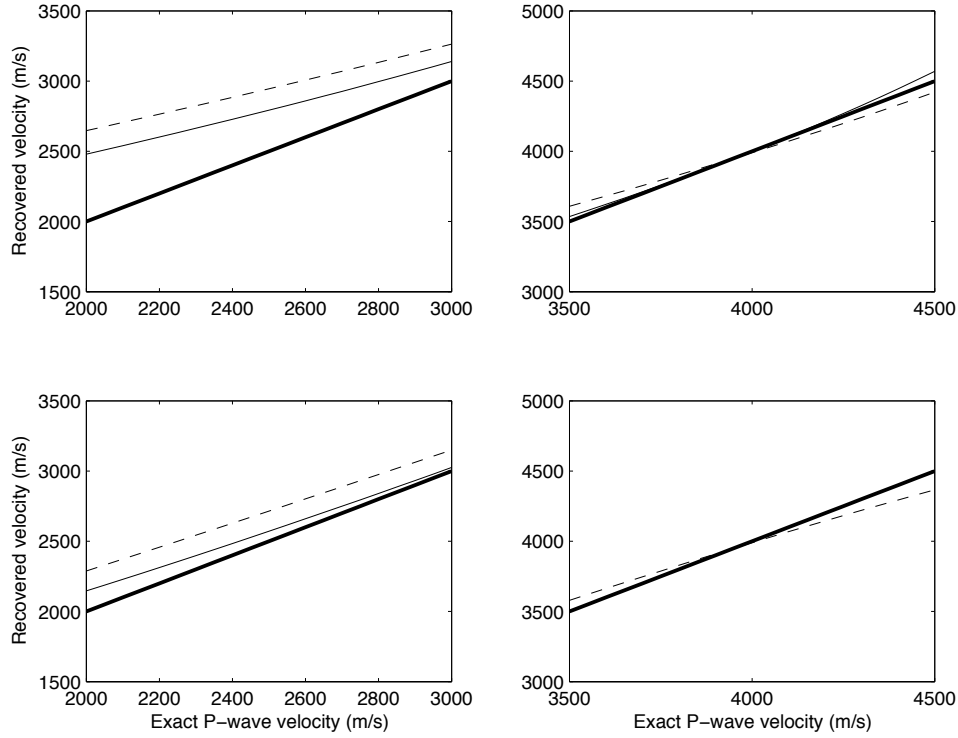


FIG. 5. Inversion comparisons for the case of the perturbed interface with $c_0 = 1500\text{m/s}$ and the baseline target P-wave velocity fixed at 3950m/s . Bold solid: exact velocity, solid: consistently posed time-lapse inversion; dashed: non time-lapse inversion. Top left: linear inversion, monitoring target velocities low compared to baseline target velocity. Top right: linear inversion, monitoring target velocities high compared to baseline target velocity. Bottom left: nonlinear inversion, low; bottom right: nonlinear inversion, high.

survey to the time of the monitoring survey. The nonlinear relationship between the difference model and the difference data (in this case, the “bump” formed from the interface step function at monitoring subtracted from the step at baseline, and the “dipole” formed from the difference of the two slightly offset primary reflections) is developed, as is the linear approximation to the relationship. This analysis forms the basis, developed in a later section, for a time-lapse specific form of imaging of differenced subsurface structures. We revisit the issue of how a non time-lapse imaging theory, which cannot account for reflections in the reference medium, to first order correctly manages a time-lapse data set.

Wave equations.

We consider waves propagating in a reference medium identical to that used in the previous problem (Figure 7, left panel), except that for the sake of later interpretation we have changed the name of the interface location from z_1 to z_I . The Green’s function therefore satisfies

$$\left[\frac{d^2}{dz^2} + \frac{\omega^2}{c_I^2(z)} \right] G(z, z_s, \omega) = \delta(z - z_s), \quad (38)$$

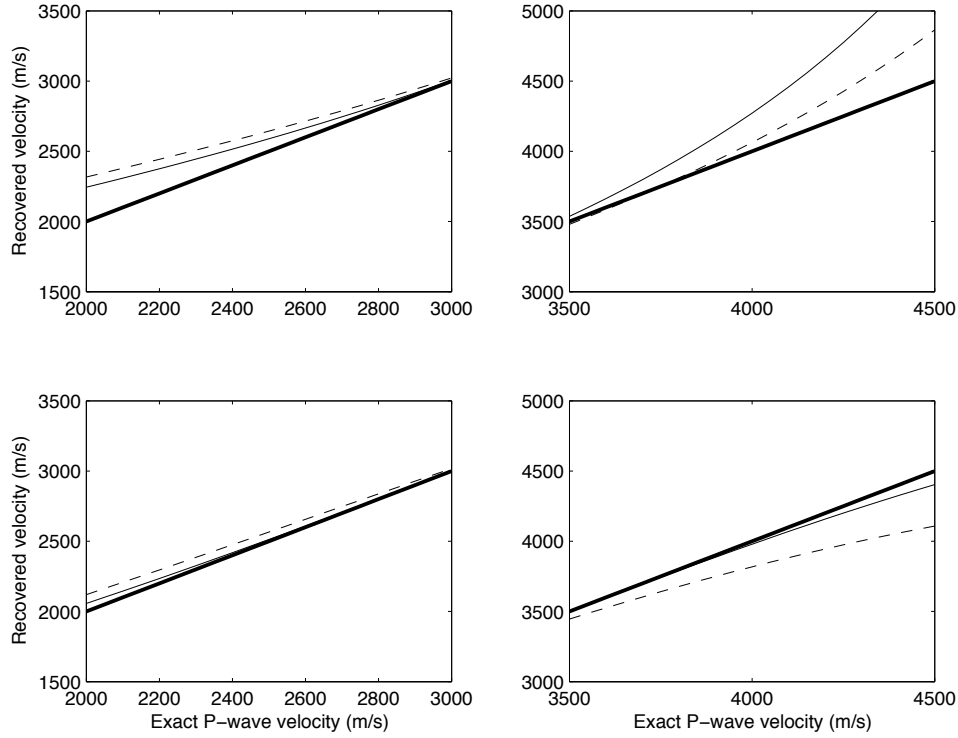


FIG. 6. Inversion comparisons for the case of the perturbed interface with $c_0 = 1500\text{m/s}$ and the baseline target P-wave velocity fixed at 3150m/s . Bold solid: exact velocity, solid: consistently posed time-lapse inversion; dashed: non time-lapse inversion. Top left: linear inversion, monitoring target velocities low compared to baseline target velocity. Top right: linear inversion, monitoring target velocities high compared to baseline target velocity. Bottom left: nonlinear inversion, low; bottom right: nonlinear inversion, high.

where

$$\frac{1}{c_I^2(z)} = \begin{cases} c_I^{-2}, & z > z_I \\ c_0^{-2}, & z < z_I \end{cases}, \quad (39)$$

with c_0 the incidence medium wavespeed and c_I the target wavespeed. We also consider a perturbed medium with the same target medium parameter value, but a boundary location altered from z_I to z_F (Figure 7, right panel), wherein the Green's function satisfies

$$\left[\frac{d^2}{dz^2} + \frac{\omega^2}{c_F^2(z)} \right] P(z, z_s, \omega) = \delta(z - z_s), \quad (40)$$

where

$$\frac{1}{c_F^2(z)} = \begin{cases} c_I^{-2}, & z > z_F \\ c_0^{-2}, & z < z_F \end{cases}. \quad (41)$$

Green's functions.

The Green's functions are the same as those used for the amplitude-perturbed interface. For the current calculation the case of $z_g, z_s < z_I$ both being within the incidence

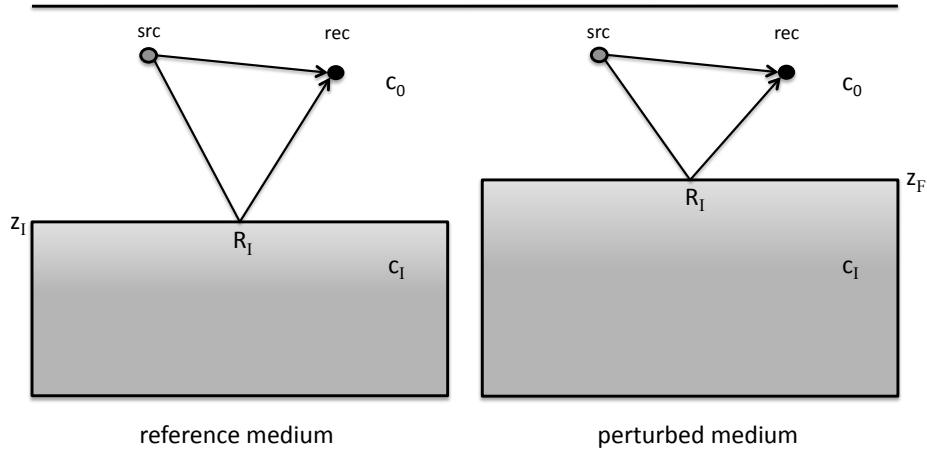


FIG. 7. Illustration of the reference and actual media in the problem of scattering from a depth-perturbed interface.

medium and an upward migrating interface is the only one needed:

$$G_{00}(z_g, z_s, \omega) = \frac{e^{ik_0|z_g-z_s|}}{i2k_0} + R_I \frac{e^{ik_0(z_I-z_g)} e^{ik_0(z_I-z_s)}}{i2k_0}, \quad (42)$$

where $k_0 = \omega/c_0$ and $R_I = (c_I - c_0)/(c_I + c_0)$. See Figure 8, left panel.

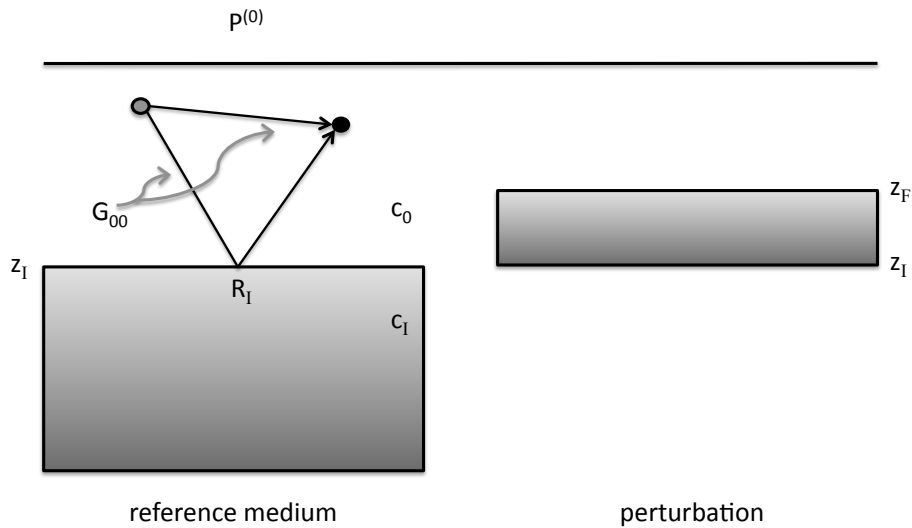


FIG. 8. Illustration of the reference medium and Green's function (left panel) and perturbation (right panel).

Solutions.

The quantity α , measuring as it does the difference between the reference and perturbed media, takes the form in this case of

$$\begin{aligned}\alpha_{TL}(z) &= 1 - \frac{c_I^2(z)}{c_F^2(z)} \\ &= \begin{cases} 0, & z < z_F \\ 1 - c_0^2/c_I^2, & z_F < z < z_I \\ 0, & z_I < z \end{cases} \quad (43) \\ &= \alpha_{TL}[H(z - z_F) - H(z - z_I)],\end{aligned}$$

where $\alpha_{TL} = 1 - c_0^2/c_I^2$ and H again represents the Heaviside function. This is the ‘‘bump’’, or pulse, we briefly examined in the Introduction (Figure 8, right panel). Forming the Born series solution for P in terms of this perturbation and the Green’s function above, we obtain

$$P(z, z_s) = P^{(0)}(z, z_s) + P^{(1)}(z, z_s) + P^{(2)}(z, z_s) + \dots, \quad (44)$$

where, setting $z_g = z_s = 0$ for convenience,

$$P^{(0)} = G_{00}(0, 0), \quad (45)$$

$$P^{(1)} = \alpha_{TL} \frac{\omega^2}{c_0^2} \int_{z_F}^{z_I} dz' G_{00}(0, z') G_{00}(z', 0) \quad (46)$$

$$P^{(2)} = \alpha_{TL}^2 k_0^4 \int_{z_F}^{z_I} dz' G_{00}(0, z') \int_{z_F}^{z_I} dz'' G_{00}(z', z'') G_{00}(z'', 0), \quad (47)$$

etc. Substituting the explicit forms for the Green’s functions we have a set of increasingly complicated contributions:

$$P^{(0)} = \frac{1}{i2k_0} + R_I \frac{e^{i2k_0 z_I}}{i2k_0}, \quad (48)$$

and

$$P^{(1)} = \frac{\alpha}{4} \frac{e^{i2k_0 z_F}}{i2k_0} - \frac{\alpha_{TL}}{4} \frac{e^{i2k_0 z_I}}{i2k_0} \left[(1 - R_I^2) + i4k_0(z_I - z_F)R_I + R_I^2 e^{i2k_0(z_I - z_F)} \right], \quad (49)$$

and

$$\begin{aligned}P^{(2)} &= \frac{\alpha_{TL}^2}{8} \frac{e^{i2k_0 z_F}}{i2k_0} - \frac{\alpha_{TL}^2}{8} \frac{e^{i2k_0 z_I}}{i2k_0} \left[\left(1 + R_I - R_I^2 - \frac{1}{2} R_I^3 \right) \right. \\ &+ 2R_I^2(i2k_0)(z_I - z_F)e^{i2k_0(z_I - z_F)} + (1 - R_I - R_I^2)R_I e^{i2k_0(z_I - z_F)} \\ &\left. + R_I(i2k_0)^2(z_I - z_F)^2 + (i2k_0)(z_I - z_F)(1 - R_I - R_I^2) + \frac{1}{2} R_I^3 e^{i4k_0(z_I - z_F)} \right], \quad (50)\end{aligned}$$

etc. The series begins to become quite complicated, but the meaning and origin of each term can be traced by sketching the propagating Green’s functions as arrows and the scattering interactions as points, as in Figure 9. Every path beginning at the source and ending at the receiver leads to one additive term in the equations for $P^{(n)}$.

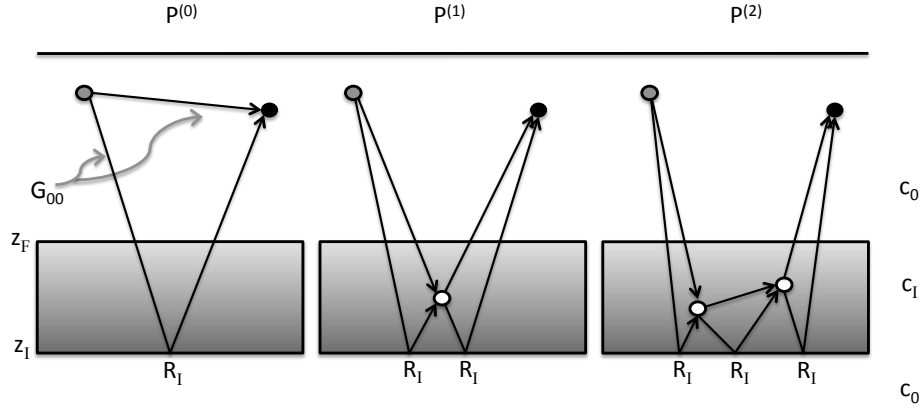


FIG. 9. An illustration of the geometry of the terms in the scattering expression in equation (44). The presence of a reflector in the reference medium increases the number of terms at each order (zero'th order in α in the left panel, first order in α_{TL} in the middle panel, and second order in α_{TL} in the right panel). Starting at the source, every combination of arrows that finishes at the receiver produces a contribution to P at that order: two at zero'th order, four at first order, etc. In contrast to the amplitude-perturbed interface case, the terms that are linear in the earlier sense (i.e., first order in α_{TL} and zero'th order in R_I) in the case of the migrating interface contain more than enough to entertain our desire for new analysis. Still, at higher order several interesting mathematical phenomena are discernible. At second order, for instance, multiple reflections are generated, reverberating between the interface and itself at the two different time-lapse survey times.

Time-lapse interpretation.

Making the identification again that α_{TL} represents the time-lapse perturbation in which a single boundary has migrated upward, we have for the difference field P_S where

$$P_S = P^{(1)} + P^{(2)} + \dots \quad (51)$$

If as before we choose to re-define the order of the solution to be due to the product of α_{TL} and R_I (as opposed to α alone, as in equation (51)), to first order we have

$$P_S \approx \frac{\alpha_{TL}}{4} \left[\frac{e^{i2k_0 z_F}}{i2k_0} - \frac{e^{i2k_0 z_I}}{i2k_0} \right]. \quad (52)$$

The two terms in the linear estimate of P_S in equation (52) have qualitatively very different origins; taken together, they will explain one of the questions raised in the introductory section of this paper. To investigate this, let us return to the solution for the perturbed field in equation (44), $P = P^{(0)} + P_S$, which was illustrated in the right panel of Figure 7. Together with equation (52), we have

$$P = \underbrace{\frac{1}{i2k_0} + R_I \frac{e^{i2k_0 z_I}}{i2k_0}}_{\text{reference field } P^{(0)}} + \underbrace{\frac{\alpha_{TL}}{4} \left[\frac{e^{i2k_0 z_F}}{i2k_0} - \frac{e^{i2k_0 z_I}}{i2k_0} \right]}_{\text{1st order correction } P^{(1)}} + \dots \quad (53)$$

The first term on the right is part of the reference field, and corresponds to the direct wave between the (co-located) source and receiver. It is a physically meaningful part of both reference and perturbed fields, and it is correctly conferred onto P directly by $P^{(0)}$. The second term on the right is the reflection from the interface z_I . This reflection occurs in

the reference medium, and is also conferred onto P by $P^{(0)}$. Unlike with the direct wave, however, this second term's presence is problematic, because there is no such event in P . If equation (53) is to produce the right answer, the only possibility is that the full series solution deletes this spurious event through the activity of the higher order terms. Consider the first order correction terms we have included. The first of these has the phase of a reflection from the perturbed depth, z_F , and is the linear term in a series constructing the (correct) single primary reflection in P . The second of these has the phase of the reference reflection, and a negative sign—it is the linear term in a second, coupled, series, whose objective is to destructively interfere with the reference reflection, extinguishing it from the final, summed, result. The total effect of both influences is the correct construction of the direct wave and the single reflected event in P .

So, when we take this series for P , and subtract from it $P^{(0)}$ to obtain the scattered field, we are left with a two-term linear expression, equation (52), whose terms look similar but have very different origins. The leftmost term represents the action of the series in constructing the desired reflection, and the rightmost in deconstructing the undesired reflection. Both are first order in α_{TL} .

A comparison with the standard scattering problem.

The full series solution for P includes, by necessity, the construction of the negative of components of the reference wave. This sheds light on why we see non time-lapse inverse scattering methods “working”, at least to first order, on time-lapse data.

As with the amplitude-perturbed example, we may conceive of a notional non time-lapse scattering problem which, in the linear approximation, generates an identical scattered field. The reflected field from a two interface (layer) model can be estimated with a standard scattering description as follows. We consider a wave at normal incidence in a homogeneous reference medium characterized by c_0 , which leads to the selection of the Green's function

$$G_0(z_g, z_s) = \frac{e^{ik_0|z_g - z_s|}}{i2k_0}, \quad (54)$$

and a perturbed medium that agrees with the reference medium everywhere except between the depths z_F and z_I , where it is characterized by c_I . Then, with the same definition for $\alpha_{TL} = 1 - c_0^2/c_I^2$ as above, we may form a linear approximation of the scattered field above both z_F and z_I using

$$\begin{aligned} P_S &\approx k_0^2 \alpha_{TL} \int_{z_F}^{z_I} G_0(0, z') G(z', 0) \\ &= \frac{\alpha_{TL}}{4} \left[\frac{e^{i2k_0 z_F}}{i2k_0} - \frac{e^{i2k_0 z_I}}{i2k_0} \right], \end{aligned} \quad (55)$$

which is equivalent to the time-lapse difference wave field in equation (52).

To first order, then, a non time-lapse scattering approximation of the field reflecting from a two-interface perturbation is equivalent to the time-lapse scattering approximation of a single mobile interface.

This provides a plausible answer the question posed in the introductory section of this paper: how could it be that standard inverse scattering methods work reasonably well when half of the events in the difference data do not exist from the point of view of the theory? The answer is, evidently, that reference reflection events associated with the reference medium, which we might purport to be nonexistent, *do* exist for time-lapse scattering because one of its tasks is the construction of the negative of all reference reflections. The appearance of the leading terms in this cancellation procedure coincide with the subtracted reference reflection events in the difference data, and, consequently, we notice the equivalence between two conceptually disparate perturbation solutions in equations (52) and (55).

A downward migrating interface.

The basic aspects of the scattering problem for an upward-migrating interface remain for the case of an interface migrating in the opposite direction. They do have differences, however, and we will briefly state them here. Because z_I and z_F effectively switch places in a re-drawing of Figure 9 to match with this case, we require Green's functions that propagate in the medium c_I as well as in c_0 . When these are incorporated and equation (46) is re-calculated for the downward migrating interface case, we have, to first order

$$\begin{aligned}
 P &\approx P^{(0)} + P^{(1)} \\
 &= \frac{1}{i2k_0} + R_I \frac{e^{i2k_0 z_I}}{i2k_0} - \frac{\alpha_{TL}}{4} \frac{c_I^2}{c_0^2} T_U T_D \left[e^{i2k_1(z_F - z_I)} \frac{e^{ik_0 z_I}}{i2k_0} - \frac{e^{i2k_0 z_I}}{i2k_0} \right]. \quad (56)
 \end{aligned}$$

Perusal of the result indicates that the basic activity remains unchanged: the process of negation of the spurious reference reflection (second term on the right hand side) is begun by the first order term at the far right, and the correct reflection is instated to first order by the third term on the right hand side. In this case, however, the negation, while approximate in amplitude, is precise in phase, whereas the correct reflection is linearly-approximate in phase also, and hence unlike the negation is prey to error at large contrast; the opposite of the behaviour seen with the upward-migrating interface. This is because the phase of any event involving propagation in perturbed regions must be determined through the nonlinear activity of the series expansion, and in switching between these two cases we have changed which interface lies beneath the perturbed region. If the time-lapse contrasts are such that the linearizations we have described are sufficiently accurate, this difference is negligible.

Linear inversion for a depth-perturbed interface.

Provided that not only are the time-lapse changes small but so are the contrasts between the baseline medium and a homogeneous background c_0 (e.g., what we referred to as α_S in equation (22)), we may pose a linear inverse problem (for 1D constant density media with data at normal incidence) to determine the difference model as follows. The data are

approximated as

$$\begin{aligned}
 D(\omega) &= P_S(0, 0) \approx \int dz' G_{00}(0, z') k_0^2 \alpha_{TL}(z') G_{00}(z', 0) \\
 &= \int dz' \left[\frac{e^{ik_0 z'}}{i2k_0} + R_I e^{-ik_0 z'} \frac{e^{i2k_0 z'}}{i2k_0} \right] k_0^2 \alpha_{TL}(z') \left[\frac{e^{ik_0 z'}}{i2k_0} + R_I e^{-ik_0 z'} \frac{e^{i2k_0 z'}}{i2k_0} \right] \\
 &\approx -\frac{1}{4} \int dz' e^{i2k_0 z'} \alpha_{TL}(z'),
 \end{aligned} \tag{57}$$

or

$$-4D(k_0) \approx \alpha_{TL}(-2k_0). \tag{58}$$

Therefore in the case of the single mobile interface we approximate the depth-wavenumber spectrum of the desired profile α_{TL} as

$$\alpha_{TL}(-2k_0) \approx -4R_I \left[\frac{e^{i2k_0 z_F}}{i2k_0} - \frac{e^{i2k_0 z_I}}{i2k_0} \right]. \tag{59}$$

In the next section we build on this analysis to develop multi-dimensional versions of the single-parameter inversion.

MULTIDIMENSIONAL IMAGING OF TIME-LAPSE DIFFERENCE DATA

Having developed some insight into a consistent formulation of the time-lapse scattering problem, we next consider the more practically meaningful problem of multidimensional time-lapse data.

Scattering from amplitude and location-varying targets

We cannot write down exact solutions for the reflecting and diffracting wave field in an arbitrarily complex baseline medium, so, by necessity there will be some mathematical (though few conceptual) differences in the detailed expressions here, as compared to the previous 1D developments. Instead we will utilize a second scattering description, with the full time-lapse problem then involving a two-level hierarchy of perturbations. Formally, we introduce three rather than two wave equations:

$$\left[\nabla^2 + \frac{\omega^2}{c_0^2(\mathbf{r})} \right] G_0(\mathbf{r}, \mathbf{r}_s) = \delta(\mathbf{r} - \mathbf{r}_s), \tag{60}$$

$$\left[\nabla^2 + \frac{\omega^2}{c_I^2(\mathbf{r})} \right] G(\mathbf{r}, \mathbf{r}_s) = \delta(\mathbf{r} - \mathbf{r}_s), \tag{61}$$

$$\left[\nabla^2 + \frac{\omega^2}{c_F^2(\mathbf{r})} \right] P(\mathbf{r}, \mathbf{r}_s) = \delta(\mathbf{r} - \mathbf{r}_s), \tag{62}$$

where $\mathbf{r} = (x, y, z)^T$, and G and P have the same time-lapse interpretation as previously, namely that they are the wave fields at the times of the baseline and monitoring surveys

respectively, and G_0 is a further reference field associated with a homogeneous background. We define a time-lapse perturbation α_{TL} that measures the difference between the media c_I and c_F as follows:

$$\alpha_{TL}(\mathbf{r}) = 1 - \frac{c_I^2(\mathbf{r})}{c_F^2(\mathbf{r})}, \quad (63)$$

and further a standard perturbation α_S that measures the difference between the medium c_I and the homogeneous background c_0 , as

$$\alpha_S(\mathbf{r}) = 1 - \frac{c_0^2(\mathbf{r})}{c_I^2(\mathbf{r})}, \quad (64)$$

From equations (61)–(62) and (63) we may form the following relationship between the baseline and monitoring fields:

$$P - G = \int d\mathbf{r}' G(\mathbf{r}, \mathbf{r}') \frac{\omega^2}{c_I^2(\mathbf{r}')} \alpha_{TL}(\mathbf{r}') P(\mathbf{r}', \mathbf{r}_s) \quad (65)$$

which is an exact expression for the difference field $P_S = P - G$. Now assuming that the reference (baseline) field G contains reflections and diffractions etc. that arise from a medium whose structure and make-up, c_I , is known, we may model these by transforming the known model c_I into α_S via equation (64), and forming a further equation for G as follows:

$$G = G_0 + \int d\mathbf{r}' G_0(\mathbf{r}, \mathbf{r}') \frac{\omega^2}{c_0^2(\mathbf{r}')} \alpha_S(\mathbf{r}') G(\mathbf{r}', \mathbf{r}_s) \quad (66)$$

Equation (66) permits $P_S = P - G$ to be represented, again exactly, through the alternative equation

$$\begin{aligned} & P_S(\mathbf{r}, \mathbf{r}_s) \\ &= \int d\mathbf{r}' \left[G_0(\mathbf{r}, \mathbf{r}') + \int d\mathbf{r}'' G_0(\mathbf{r}, \mathbf{r}'') \frac{\omega^2}{c_0^2(\mathbf{r}'')} \alpha_S(\mathbf{r}'') G(\mathbf{r}'', \mathbf{r}') \right] \frac{\omega^2}{c_I^2(\mathbf{r}')} \alpha_{TL}(\mathbf{r}') P(\mathbf{r}', \mathbf{r}_s). \end{aligned} \quad (67)$$

The analogue, in this three dimensional milieu, to the choice we made in 1D of defining the order of a given term to correspond to the combined order of α and R_I , is to define here the order of a term to be $M + N$ if the term is M 'th order in α_{TL} and N 'th order in α_S . With that in mind, linearization of equation (67) requires, first, that P be replaced by its zeroth order term in α_{TL} , namely G , second, that all instances of G be replaced by their zeroth order terms in α_S , namely G_0 , and third, that only first order terms, in the sense we have just decided upon, be retained. This results in

$$P_S(\mathbf{r}, \mathbf{r}_s) \approx \int d\mathbf{r}' G_0(\mathbf{r}, \mathbf{r}') \frac{\omega^2}{c_0^2(\mathbf{r}')} \alpha_{TL}(\mathbf{r}') G_0(\mathbf{r}', \mathbf{r}_s). \quad (68)$$

Perusal of equation (68) confirms that our earlier conclusion (in the 1D analysis) remains unchanged, namely, that although the difference field P_S , when expressed in exact integral

form, is seen to be significantly influenced by the reflections and diffractions present in the baseline survey data, to first order (i.e., when the medium perturbations giving rise to both initial reflections in the baseline survey and changes between the baseline survey and the monitoring survey are small) only the time-lapse perturbation contributes significantly to P_S . And, the approximate expression for P_S again may be interpreted in two ways: either as the difference field of the time lapse survey, or as the scattered field associated with the totally fictional wave experiment depicted in Figure 10. In this second interpretation, waves propagate everywhere in a homogeneous medium given by c_0 , and scatter from volume inclusions α_{TL} , which, we recall, correspond not to any real medium but rather to the differenced medium in the time-lapse sense.

Equation (68) also confirms again that if standard imaging and inversion algorithms are applied apparently ad hoc to the difference data associated with the time-lapse problem, to first order, i.e., if all perturbations are small, the correct difference model will be obtained.

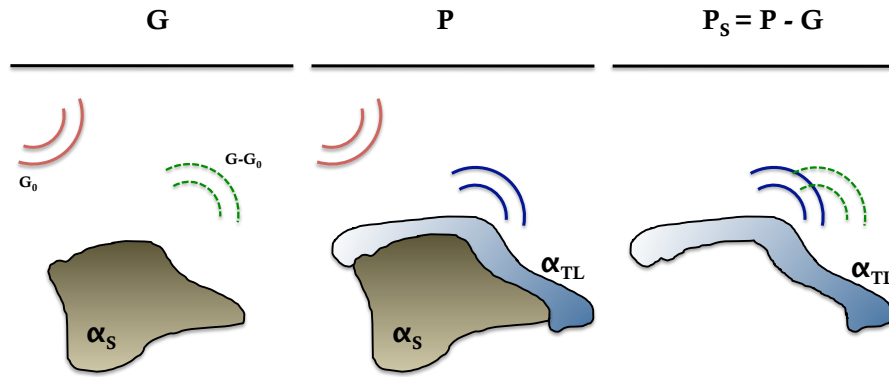


FIG. 10. An illustration of the multidimensional time-lapse scattering problem. To first order, the difference model α_{TL} is related to the difference data P_S as if it were a physical target embedded alone in the background reference medium. To second order and higher, the amplitudes of the scattered field are nonlinearly related to the difference model and the amplitudes in the baseline data amplitudes G . The perturbation framework we are setting out limits the model contrasts within which standard imaging algorithms may be applied to difference data, and provides corrective procedures for determining model parameters that lie outside those limits.

Multidimensional imaging of time-lapse difference data

The model embodied in equation (68) leads to a range of approaches for inversion. We will consider the direct solution for the difference model, and a least-squares casting of the problem.

Direct imaging

Equation (68) is a pipeline, as it were, to existing direct linearized imaging/inversion algorithms (e.g., Clayton and Stolt, 1981; Beylkin, 1985; Bleistein et al., 2000). For instance, consider the case of a 2D Earth and a homogeneous reference medium with wavespeed c_0 . We associate the data $D(k_g, k_s, \omega)$ with the scattered field P_S projected onto a measurement surface $z = 0$, (with source and receiver depths also at the origin), and

assume $\alpha_{TL} = 0$ at and above this level. The coordinates k_g and k_s are the Fourier conjugates to source and receiver coordinates x_g, x_s . In a direct extension of equation (59), and following Clayton and Stolt (1981), we relate the spectrum of the perturbation with the spectrum of the data:

$$\alpha_{TL}(k_m, k_z) = -4 \frac{q_g q_s c_0^2}{\omega^2} D(k_g, k_s, \omega), \quad (69)$$

where

$$\begin{aligned} k_m &= k_g - k_s, \\ k_z &= -q_g - q_s, \\ q_g &= \frac{\omega}{c_0} \sqrt{1 - \frac{k_g^2 c_0^2}{\omega^2}}, \\ q_s &= \frac{\omega}{c_0} \sqrt{1 - \frac{k_s^2 c_0^2}{\omega^2}}, \end{aligned} \quad (70)$$

and k_m is the Fourier conjugate to the lateral (x) model coordinate and k_z is conjugate to the depth (z) model coordinate. If the time-lapse alteration, for instance due to steam-heating of a reservoir target, has included the introduction of an anelastic/viscoelastic behaviour in the perturbation, the inverse procedure of Innanen and Weglein (2007) may instead be implemented.

A least-squares approach

Equation (68) leads to a data model of the form

$$D(\mathbf{r}, \mathbf{r}_S) = \int d\mathbf{r}' G_0(\mathbf{r}, \mathbf{r}') \frac{\omega^2}{c_I^2(\mathbf{r}')} \alpha_{TL}(\mathbf{r}') G_0(\mathbf{r}', \mathbf{r}_S), \quad (71)$$

which has been used in a least-squares sense to solve standard seismic imaging and interpolation problems allowing for sampling, aperture and various other limitations of field data (Kaplan et al., 2010b,a). In a companion paper to this one we explore the time-lapse version of this data model and comment on its ability to cope with registration and repeatability issues of practical importance to field implementation (Naghizadeh and Innanen, 2010).

MULTIPARAMETER INVERSION OF TIME-LAPSE DIFFERENCE REFLECTIVITY

In the initial analysis section, we demonstrated how the difference reflection coefficient due to a variation in the impedance in a scalar medium at normal incidence could be (1) directly expanded in series about the time-lapse perturbation and orders of the baseline reflection coefficient, and (2) directly inverted through an order-by-order procedure. In this section we apply this approach to determine time-lapse variations in multiple parameters at a single, isolated interface, using the variation of the difference reflection coefficient with angle and/or frequency. The purpose here is to demonstrate the idea in principle; more complete multiparameter schemes follow with additional algebraic, but not conceptual, complexity.

Inversion for P-wave velocity and Q time lapse variations using the frequency variability of the difference reflection coefficient

Let us analyze the following inverse time-lapse problem. An acoustic/elastic boundary across which P-wave velocity varies from c_0 to c_I , at the time of the baseline survey, is subject to some production process involving perhaps of fluid or steam injection. Over calendar time, the target (lower) medium varies in its P-wave velocity, from c_I to c_F , and in addition takes on a viscous or dissipative component with a finite quality factor Q_F . If the dissipative medium is such that the wave propagation constant is given by

$$K = \frac{\omega}{c} \left[1 + \frac{F(\omega)}{Q_F} \right], \quad (72)$$

$$F(\omega) = \frac{i}{2} - \frac{1}{\pi} \log \left(\frac{\omega}{\omega_0} \right),$$

as discussed for instance by (Aki and Richards, 2002), then determine c_F and Q_F from measurements of the difference reflection coefficient at normal incidence:

$$R_S(\omega) = R_F(\omega) - R_I$$

$$= \frac{1 - \frac{c_0}{c_F} \left[1 + \frac{F(\omega)}{Q_F} \right]}{1 + \frac{c_0}{c_F} \left[1 + \frac{F(\omega)}{Q_F} \right]} - R_I \quad (73)$$

$$= \frac{1 - \left(\frac{c_0}{c_I} \right) \left(\frac{c_I}{c_F} \right) \left[1 + \frac{F(\omega)}{Q_F} \right]}{1 + \left(\frac{c_0}{c_I} \right) \left(\frac{c_I}{c_F} \right) \left[1 + \frac{F(\omega)}{Q_F} \right]} - R_I,$$

where

$$R_I = \frac{1 - \frac{c_0}{c_I}}{1 + \frac{c_0}{c_I}}. \quad (74)$$

We solve this by extending the previous analysis on direct expansion and inversion of time-lapse reflectivity. Defining time-lapse perturbations

$$\alpha_c^{TL} = 1 - \frac{c_I^2}{c_F^2} \quad (75)$$

$$\alpha_Q^{TL} = 1/Q_F,$$

and the baseline or standard perturbation

$$\alpha_c^S = 1 - \frac{c_0^2}{c_I^2}, \quad (76)$$

substituting into equation (73) and expanding, we have

$$R_S(\omega) = \left(\frac{1}{4} \alpha_c^{TL} - \frac{1}{2} F(\omega) \alpha_Q^{TL} \right) + \left(\frac{1}{8} \alpha_c^{TL^2} + \frac{1}{4} F^2(\omega) \alpha_Q^{TL^2} \right)$$

$$+ \left(\frac{1}{4} \alpha_c^S + \frac{1}{8} \alpha_c^{S^2} \right) - \alpha_c^S \left(\frac{1}{64} \alpha_c^{TL^2} - \frac{1}{16} F(\omega) \alpha_Q^{TL} \alpha_c^{TL} + \frac{1}{16} F^2(\omega) \alpha_Q^{TL^2} \right) \quad (77)$$

$$- \alpha_c^{S^2} \left(\frac{1}{64} \alpha_c^{TL} - \frac{1}{32} F(\omega) \alpha_Q^{TL} \right) + \dots - R_I.$$

The third bracketed term on the right hand side, containing only powers of α_c^S , is interpreted as a series for the construction of R_I , and ultimately this term and the last term in equation (77) negate one another. Furthermore, as in the initial analysis section of this paper, we may replace the baseline/standard perturbation with its expansion in orders of the baseline reflection coefficient: $\alpha_c^S = 4R_I - 8R_I^2 + 12R_I^3 - \dots$, leaving

$$R_S(\omega) = \frac{1}{4}\alpha_c^{TL}(1 - R_I^2) - \frac{1}{2}F(\omega)\alpha_Q^{TL}(1 - R_I^2) + \frac{1}{8}\alpha_c^{TL^2} \left(1 - \frac{1}{2}R_I + R_I^2\right) + \frac{1}{4}F^2(\omega)\alpha_Q^{TL^2}(1 - R_I + 2R_I^2) + \frac{1}{4}F(\omega)\alpha_Q^{TL}\alpha_c^{TL}(R_I - 2R_I^2) + \dots \quad (78)$$

Inversion is carried out as in equation (35) with the slight complication that N parameters require at least N data (i.e., R_S values at N frequencies); this is discussed for non time-lapse problems by (Innanen, 2010). Forming inverse series

$$\begin{aligned} \alpha_c^{TL} &= \alpha_{c_1}^{TL} + \alpha_{c_2}^{TL} + \dots, \\ \alpha_Q^{TL} &= \alpha_{Q_1}^{TL} + \alpha_{Q_2}^{TL} + \dots, \end{aligned} \quad (79)$$

where subscript i indicates that the term is i th order in R_S , substituting these into equation (78), equating like orders, and sequentially determining each term, we obtain the solution to first order:

$$\begin{aligned} \alpha_{c_1}^{TL} &= -4 \frac{F(\omega_2)\mathcal{R}_S(\omega_1) - F(\omega_1)\mathcal{R}_S(\omega_2)}{F(\omega_2) - F(\omega_1)}, \\ \alpha_{Q_1}^{TL} &= -2 \frac{\mathcal{R}_S(\omega_1) - \mathcal{R}_S(\omega_2)}{F(\omega_2) - F(\omega_1)}, \end{aligned} \quad (80)$$

or exactly, in series form, as

$$\begin{aligned} \alpha_c^{TL} &= -4 \left(\frac{F_2\mathcal{R}_S(\omega_1) - F_1\mathcal{R}_S(\omega_2)}{F_2 - F_1} + \frac{F_2\mathcal{M}(\omega_1) - F_1\mathcal{M}(\omega_2)}{F_2 - F_1} + \dots \right), \\ \alpha_Q^{TL} &= -2 \left(\frac{\mathcal{R}_S(\omega_1) - \mathcal{R}_S(\omega_2)}{F_2 - F_1} + \frac{\mathcal{M}(\omega_1) - \mathcal{M}(\omega_2)}{F_2 - F_1} + \dots \right), \end{aligned} \quad (81)$$

where $F_i = F(\omega_i)$,

$$\mathcal{R}_S(\omega) = \frac{R_S(\omega)}{1 - R_I^2}, \quad \mathcal{M}(\omega) = \frac{M(\omega)}{1 - R_I^2}, \quad (82)$$

and

$$\begin{aligned} M(\omega) &= -\frac{1}{8}\alpha_{c_1}^{TL^2} \left(1 - \frac{1}{2}R_I + R_I^2\right) - \frac{1}{4}F^2(\omega)\alpha_{Q_1}^{TL^2}(1 - R_I + 2R_I^2) \\ &\quad - \frac{1}{4}F(\omega)\alpha_{Q_1}^{TL}\alpha_{c_1}^{TL}(R_I - 2R_I^2). \end{aligned} \quad (83)$$

From these perturbations the target properties c_F and Q_F are recovered. As ever in this theory, the difference between the time-lapse inversion and the results that would have been attained by applying inverse scattering or inverse series algorithms derived without time-lapse assumptions, is the presence of R_I terms. Setting these to zero throughout recovers nontime-lapse algorithm forms.

Inversion for P-wave velocity and density time lapse variations using the angle variability of the difference reflection coefficient

In non time-lapse seismic AVA (amplitude variation with angle) analysis, angle variations in the reflection coefficient can distinguish between density and velocity variations at a subsurface boundary. The same is true of the difference reflection coefficient in the time-lapse problem. Consider a baseline target whose density and P-wave velocity undergo a contrast from c_0, ρ_0 to c_I, ρ_I . Over calendar time, the properties of the lower medium both change from c_I, ρ_I to c_F, ρ_F . This leads to a difference reflection coefficient

$$R_S(\theta) = R_F(\theta) - R_I(\theta) = \frac{1 - \Omega}{1 + \Omega} - R_I(\theta), \quad (84)$$

where

$$R_I(\theta) = \frac{c_I \rho_I \cos \theta - c_0 \rho_0 \sqrt{1 - \frac{c_I^2}{c_0^2} \sin^2 \theta}}{c_I \rho_I \cos \theta + c_0 \rho_0 \sqrt{1 - \frac{c_I^2}{c_0^2} \sin^2 \theta}}, \quad (85)$$

and, for small θ ,

$$\Omega = \left(\frac{\rho_0}{\rho_I} \frac{\rho_I}{\rho_F} \right) \left(\frac{c_0}{c_I} \frac{c_I}{c_F} \right) \left[1 - \frac{1}{2} \left(\frac{c_I}{c_0} \right)^2 \left(\frac{c_F}{c_I} \right)^2 \sin^2 \theta \right] \left(1 + \frac{1}{2} \sin^2 \theta \right). \quad (86)$$

(The small angle approximation is convenient but not critical here, being based on the binomial series expansion and linearization of two radical functions. Those expansions may be truncated at higher order, and in principle for any $\theta < \pi/2$, to maintain desired accuracy.) The problem is to determine c_F and ρ_F from known baseline properties and measurements of R_S . As before we begin by direct expansion of the difference reflection coefficient. Defining baseline/standard and time-lapse perturbations

$$\begin{aligned} \alpha_c^{TL} &= 1 - \frac{c_I^2}{c_F^2}, & \alpha_\rho^{TL} &= 1 - \frac{\rho_I}{\rho_F}, \\ \alpha_c^S &= 1 - \frac{c_0^2}{c_I^2}, & \alpha_\rho^S &= 1 - \frac{\rho_0}{\rho_I}, \end{aligned} \quad (87)$$

substituting these into equation (86) and expanding, we obtain

$$\begin{aligned} R_S(\theta) &= \left[\frac{1}{4}(1 + \sin^2 \theta) \alpha_c^{TL} + \frac{1}{2} \alpha_\rho^{TL} \right] + \left[\frac{1}{8}(1 + 2 \sin^2 \theta) \alpha_c^{TL^2} + \frac{1}{4} \alpha_\rho^{TL^2} \right] \\ &+ \left[\frac{1}{4}(1 + \sin^2 \theta) \alpha_c^S + \frac{1}{2} \alpha_\rho^S \right] + \left[\frac{1}{8}(1 + 2 \sin^2 \theta) \alpha_c^{S^2} + \frac{1}{4} \alpha_\rho^{S^2} \right] \\ &+ \frac{1}{4} \alpha_c^S \alpha_c^{TL} \sin^2 \theta + \dots - R_I(\theta), \end{aligned} \quad (88)$$

where the ellipsis indicates terms at third order and higher an any combination of the perturbations. Once again we interpret the series terms on the second line of equation (88) as working to construct the baseline reflection coefficient, which is then negated by the last

term in the expression. The question we must cope with here is how to replace *two* sets of baseline perturbations, α_c^S and α_ρ^S , with baseline wave information, ideally $R_I(\theta)$. We proceed as follows. Expanding and inverting expressions for reflection coefficients R_c and R_ρ , where

$$\begin{aligned} R_I^c &= \frac{c_I - c_0}{c_I + c_0}, \\ R_I^\rho &= \frac{\rho_1 - \rho_0}{\rho_1 + \rho_0}, \end{aligned} \quad (89)$$

we have the two relationships

$$\begin{aligned} \alpha_c^S &= 4R_I^c - 8R_I^{c2} + 12R_I^{c3} - \dots \\ \alpha_\rho^S &= 2R_I^\rho - 2R_I^{\rho2} + 2R_I^{\rho3} - \dots \end{aligned} \quad (90)$$

Upon substitution into equation (88) we obtain

$$\begin{aligned} R_S(\theta) &= \frac{1}{4}\alpha_c^{TL} [1 - (R_I^c + R_I^\rho)^2] + \frac{1}{2}\alpha_\rho^{TL} [1 - (R_I^c + R_I^\rho)^2] \\ &+ \frac{1}{4}\alpha_c^{TL} \left[1 - R_I^{\rho2} + \frac{5}{4}R_I^{c2} + R_I^c - R_I^\rho R_I^c \right] \sin^2 \theta \\ &- \alpha_\rho^{TL} [R_I^{c2} + R_I^\rho R_I^c] \sin^2 \theta + \dots \end{aligned} \quad (91)$$

Since to third order in the individual reflection coefficients $R_I \approx R_I^c + R_I^\rho$, we may express the normal incidence terms as functions of R_I directly. Some of the factors of $\sin^2 \theta$ may also be expressed this way, with a remainder in terms of the two individual coefficients:

$$\begin{aligned} R_S(\theta) &= \left[\frac{1}{4}\alpha_c^{TL} + \frac{1}{2}\alpha_\rho^{TL} \right] [1 - R_I^2(\theta)] + \frac{1}{4}\alpha_c^{TL} [1 + R_I(\theta) - R_I^2(\theta)] \sin^2 \theta \\ &+ \frac{1}{4}\alpha_c^{TL}(A + B) \sin^2 \theta - \alpha_\rho^{TL} B \sin^2 \theta + \dots, \end{aligned} \quad (92)$$

where $A = 2R_I^{c2}$ and $B = -R_I^{\rho2}(1 - R_I^c)$. When it comes to inversion in principle the baseline medium is assumed to be known, and hence A and B can be straightforwardly synthesized. The next step is to form inverse series

$$\begin{aligned} \alpha_c^{TL} &= \alpha_{c_1}^{TL} + \alpha_{c_2}^{TL} + \dots, \\ \alpha_\rho^{TL} &= \alpha_{\rho_1}^{TL} + \alpha_{\rho_2}^{TL} + \dots, \end{aligned} \quad (93)$$

where as before subscript i indicates that the term is i th order in R_S , substitute and sequentially solve for terms to approximate the perturbations. Let us demonstrate within the linear (in $\alpha_c^{TL}, \alpha_\rho^{TL}$) regime; nonlinear correction occurs as in the previous section. We have

$$\mathcal{R}_S(\theta) \approx \frac{1}{2}\alpha_\rho^{TL} + \frac{1}{4}\mathcal{G}(\theta)\alpha_c^{TL}, \quad (94)$$

where

$$\begin{aligned} \mathcal{R}_S(\theta) &= H^{-1}(\theta)R_S(\theta), \\ \mathcal{G}(\theta) &= H^{-1}(\theta)[1 - R_I^2(\theta)] + H^{-1}(\theta)[1 + R_I(\theta) - R_I^2(\theta) + A + B] \sin^2 \theta, \end{aligned} \quad (95)$$

and

$$H(\theta) = 1 - R_I^2(\theta) - 2B \sin^2 \theta, \quad (96)$$

in which case

$$\begin{aligned} \alpha_c^{TL} &\approx 4 \frac{\mathcal{R}_S(\theta_1) - \mathcal{R}_S(\theta_2)}{\mathcal{G}(\theta_1) - \mathcal{G}(\theta_2)} \\ \alpha_\rho^{TL} &\approx 2 \frac{\mathcal{G}(\theta_2)\mathcal{R}_S(\theta_1) - \mathcal{G}(\theta_1)\mathcal{R}_S(\theta_2)}{\mathcal{G}(\theta_1) - \mathcal{G}(\theta_2)} \end{aligned} \quad (97)$$

given data at two angles.

CONCLUSIONS: DIFFERENCE MODELS/DATA AND WAVE PHYSICS

Let us try to make the relevance of what we have done here clearer, by taking a step back and considering the bigger picture. Our interest is to estimate the changes a volume of the Earth undergoes in the relative short-term, e.g., during a hydrocarbon production or gas/fluid injection process, or in the relative long-term, e.g., during monitoring of CO₂ storage. This is achieved by inverting the calendar-time variation of the Earth volume’s seismic response. For a geophysicist working in the second decade of the 21st century, in thinking of any sort of seismic inversion the inclination is to pursue a maximally “physical” approach, akin to full waveform inversion, in which the parameters of interest are connected to the data through as complete as possible a wave equation[†].

The issue is, in the time-lapse problem the parameters of interest measure the *change* in a medium: they are *difference* parameters. But what does it mean to propagate a wave physically through a *difference* model? Let us through discussion predict some of the results of a numerical survey of the propagation of waves through such models.

The first thing we would find is that the basic tenets of the problem steer us inexorably towards the use of a perturbation description. That is, we encounter immediate problems if we do not frame the difference model in terms of a fixed background medium which the baseline and monitoring media each perturb. If we attempt to quantify waves propagating through absolute model differences, large fractions of the model space will have zero wave velocity. Framing the difference model as a *difference of perturbations*, as we have in this paper, is less of a choice than it might seem.

This is encapsulated in the the difference model in the bottom right panel of Figure 1. Next let us imagine propagating a wave through this difference model with the full (2-way) wave equation. Some of the reflected events will indeed correspond to those in the difference data pictured in the bottom middle panel of Figure 1. However, others will not—one thing we must expect to see are a train of reverberations or multiple reflections from within the difference layer. These events are spurious from the point of view of the

[†]By which we mean including as few of the standard approximations as possible. Examples of approximations most full waveform inversion methods exclude are one-way, or paraxial, approximations, and high frequency or ray approximations.

difference data, and are indeed nonphysical, corresponding to reflections between a single interface and *itself* at an earlier time.

These spurious multiples and other figments of the difference model/difference data relationship are part of the current framework too. Indeed in equation (50) and in the right panel of Figure 9 the low order terms in the construction of such multiple reflections are already encountered. The difference between the scattering model and the full-wave approach we have been discussing is that (1) the full series also creates terms which destructively interfere with these spurious multiples, as it does for all components of the field involving reference medium wave components (e.g., Matson, 1996), and (2) in any case through selective or partial summation (Innanen, 2009) we may avoid incorporating spurious or redundant entities (i.e., quantities such as spurious multiples which are added then subtracted by the “raw” scattering series) in any modeling or inversion scheme we choose. A straight linearization, as in the previous section, is the simplest way of suppressing such spurious events.

In summary, a range of disparate issues appear to combine to favour a scattering or perturbation treatment of the time-lapse problem. It provides a way of relating the difference model to the difference data in a way that incorporates full wave physics; also, it encounters none of the fundamental obstacles in forming such relationships we must expect from other wave-theoretic modeling and inversion approaches. If we consider an inversion of the reflectivity associated with a single boundary, that is either motionless on the time-lapse scale or has been successfully registered, formulas for estimation of multiple Earth mechanical properties can be straightforwardly derived by direct expansion of the difference reflection coefficient followed by order-by-order inversion. If we consider global changes in structure within the Earth volume of interest, remaining in the linearized regime leads also to straightforward algorithms for the imaging of differences. Practical numerical and algorithmic treatment of that problem is the subject of the companion paper to this one (Naghizadeh and Innanen, 2010).

REFERENCES

- Aki, K., and Richards, P. G., 2002, *Quantitative Seismology*: University Science Books, 2nd edn.
- Arts, R., Eiken, O., Chadwick, A., Zweigel, P., van der Meer, L., and Zinszner, B., 2004, Monitoring of CO₂ injected at Sleipner using time-lapse seismic data: *Energy*, **29**, 1383–1392.
- Ayeni, G., and Biondi, B., 2010, Target-oriented joint least-squares migration/inversion of time-lapse seismic data sets: *Geophysics*, **75**, No. 3, R61–R73.
- Berkhout, A. J., and Verschuur, D. J., 2007, Time lapse processing in the inverse data space, *in* *Proceedings of the 77th Annual Meeting of the Society of Exploration Geophysicists*, San Antonio, TX, Soc. Expl. Geophys.
- Beylkin, G., 1985, Imaging of discontinuities in the inverse scattering problem by inversion of a causal generalized radon transform: *J. Math. Phys.*, **26**, 99–108.

- Bleistein, N., Cohen, J. K., and Stockwell, J. W., 2000, *Mathematics of multidimensional seismic imaging, migration and inversion*: Springer-Verlag.
- Clayton, R. W., and Stolt, R. H., 1981, A Born-WKBJ inversion method for acoustic reflection data: *Geophysics*, **46**, No. 11, 1559–1567.
- Fomel, S., and Jin, L., 2009, Time-lapse image registration using the local similarity attribute: *Geophysics*, **74**, No. 2, A7–A11.
- Greaves, R. J., and Fulp, T. J., 1987, Three-dimensional seismic monitoring of an enhanced oil recovery process: *Geophysics*, **52**, No. 9, 1175–1187.
- Innanen, K. A., 2008, A direct non-linear inversion of primary wave data reflecting from extended, heterogeneous media: *Inverse Problems*, , No. 24, 035,021.
- Innanen, K. A., 2009, Born series forward modeling of seismic primary and multiple reflections: an inverse scattering shortcut: *Geophys. J. Int.*, **177**, No. 3, 1197–1204.
- Innanen, K. A., 2010, Inversion of the seismic AVF/AVA signatures of highly attenuative targets: Submitted to *Geophysics*.
- Innanen, K. A., and Weglein, A. B., 2007, On the construction of an absorptive-dispersive medium model via direct linear inversion of reflected seismic primaries: *Inverse Problems*, , No. 23, 2289–2310.
- Kaplan, S. T., Naghizadeh, M., and Sacchi, M. D., 2010a, Data reconstruction with shot-profile least-squares migration: *Geophysics*, **75**.
- Kaplan, S. T., Routh, P. S., and Sacchi, M. D., 2010b, Derivation of forward and adjoint operators for least-squares shot-profile migration: *Geophysics*, **75**, No. 6.
- Landro, M., 2001, Discrimination between pressure and fluid saturation changes from time-lapse seismic data: *Geophysics*, **66**, No. 3, 836–844.
- Lumley, D., 2001, Time-lapse seismic reservoir monitoring: *Geophysics*, **66**, No. 1, 50–53.
- Matson, K. H., 1996, The relationship between scattering theory and the primaries and multiples of reflection seismic data: *Journal of Seismic Exploration*, **5**, 63–78.
- Naghizadeh, M., and Innanen, K. A., 2010, A least-squares shot-profile application of time-lapse inverse scattering: *CREWES Annual Report*.
- Stucci, E., Mazzotti, A., and Ciutti, S., 2005, Seismic preprocessing and amplitude cross-calibration for a time-lapse amplitude study on seismic data from the Oseberg reservoir: *Geophysical Prospecting*, **53**, 265–282.
- Weglein, A. B., Araújo, F. V., Carvalho, P. M., Stolt, R. H., Matson, K. H., Coates, R. T., Corrigan, D., Foster, D. J., Shaw, S. A., and Zhang, H., 2003, Inverse scattering series and seismic exploration: *Inverse Problems*, , No. 19, R27–R83.

Winthaege, P. L. A., Verschuur, D. J., and Berkhout, A. J., 2004, Use of data-driven focusing operators for a quantitative approach to time lapse seismic, *in* Proceedings of the EAGE, Paris, France, Eur. Ass. Geosci. Eng.

Zhang, H., 2006, Direct non-linear acoustic and elastic inversion: towards fundamentally new comprehensive and realistic target identification: Ph.D. thesis, University of Houston.

Zhang, H., and Weglein, A. B., 2009a, Direct nonlinear inversion of multiparameter 1D acoustic media using inverse scattering subseries: *Geophysics*, **74**, No. 6, WCD29–WCD39.

Zhang, H., and Weglein, A. B., 2009b, Direct nonlinear inversion of multiparameter 1D elastic media using the inverse scattering series: *Geophysics*, **74**, No. 6, WCD15–WCD27.